# Chapter 19

# Cell-Specific RNA Quantification in Human SN DA Neurons from Heterogeneous *Post-mortem* Midbrain Samples by UV-Laser Microdissection and RT-qPCR

**Johanna Duda, Michael Fauler, Jan Gründemann, and Birgit Liss**

## Abstract

Cell specificity of gene expression analysis is from particular relevance when the abundance of target cells is not homogeneous in the compared tissue samples, like it is the case, e.g., when comparing brain tissues from controls and in neurodegenerative disease states. While single-cell gene expression profiling is already a methodological challenge per se, it becomes even more prone to artifacts when analyzing individual cells from human *post-mortem* samples. Not only because human samples can never be matched as precisely as those from animal models, but also, because the RNA-quality that can be obtained from human samples usually displays a high range of variability. Here, we detail our most actual method for combining contact-free UV-laser microdissection (UV-LMD) with reverse transcription and quantitative PCR (RT-qPCR) that addresses all these issues. We specifically optimized our protocols to quantify and compare mRNA as well as miRNA levels in human neurons from *post-mortem* brain tissue. As human *post-mortem* tissue samples are never perfectly matched (e.g., in respect to distinct donor ages and RNA integrity numbers RIN), we refined data analysis by applying a linear mixed effects model to RT-qPCR data, which allows dissecting and subtracting linear contributions of distinct confounders on detected gene expression levels (i.e., RIN, age). All these issues were considered for comparative gene expression analysis in dopamine (DA) midbrain neurons of the *Substantia nigra* (SN) from controls and Parkinson's disease (PD) specimens, as the preferential degeneration of SN DA neurons in the pathological hallmark of PD. By utilizing the here-described protocol we identified that a variety of genes—encoding for ion channels, dopamine metabolism proteins, and PARK gene products—display a transcriptional dysregulation in remaining human SN DA neurons from PD brains compared to those of controls. We show that the linear mixed effects model allows further stratification of RT-qPCR data, as it indicated that differential gene expression of some genes was rather correlated with different ages of the analyzed human brain samples than with the disease state.

**Key words** UV-laser microdissection, Single cells, Real-time quantitative PCR, Reverse transcription, *Post-mortem* human tissue, Non-optimally matched human samples, RNA integrity number RIN, Random primer, Oligo-dT primer, miScript, microRNA, Linear mixed effects model, Parkinson's disease, Dopamine

Graeme I. Murray (ed.), *Laser Capture Microdissection: Methods and Protocols*, Methods in Molecular Biology, vol. 1723,
https://doi.org/10.1007/978-1-4939-7558-7_19, 

## 1 Introduction

Quantitative real-time PCR of reverse transcribed RNA (RT-qPCR) is still a gold standard for gene expression analysis of desired target genes [1, 2]. Also for global comparison of gene expression, e.g., via RNA-Seq and related techniques, single-cell resolution is a desired goal [3–7]. Transcriptional cell-to-cell variations—depending on cell cycle, epigenetics or unknown, potentially stochastic events—as well as disease-related variations might be masked if probes are not sampled on the level of identified individual cells [8, 9]. Furthermore, not only the differential expression of target genes might vary between control and disease samples, but also the composition of the tissue itself. In neurodegenerative diseases for instance, high levels of cellular heterogeneity, selective neuron loss, and disease-related changes in non-neuronal cells will contribute to an altered composition of the diseased brain tissue compared with that in control brains [10–12]. This will confound conclusions about specific gene expression changes in the cell type of interest.

The second most common neurodegenerative disease, Parkinson's disease (PD), provides a concrete example: one of the key pathological hallmarks of PD brains and its animal models is the substantial loss of dopamine containing (DA) midbrain neurons within the *Substantia nigra pars compacta* (SN) [13–16]. In PD, clinical motor symptoms manifest only when already about 75% of these DA midbrain neurons—the most prominent cell type within the SN—are lost [17, 18]. This massive loss of SN DA neurons will confound mRNA expression analysis of PD midbrain tissue when compared to tissue samples from control non-PD brains, simply because the number of SN DA neurons in PD and control midbrain tissue samples varies immensely. Furthermore, gene expression analysis at the level of PD midbrain tissue will be distorted by the altered numbers and functional states of non-neuronal cells like microglia, astrocytes, and local T-cells, known to change in PD [19]. And finally the midbrain contains different types of DA neurons that are affected differentially by degeneration in PD: while SN DA neurons are highly vulnerable to PD-stressors, neighboring DA midbrain neurons in the ventral tegmental arear remain largely resistant [20]. All these factors could explain the large number of different and even contrary findings of tissue-based gene expression studies in PD brains; e.g., for α-synuclein [reviewed in [21]]—a gene that can cause familial forms of PD when mutated (PARK1) or duplicated/triplicated (PARK4) [22–25]. Cell-specific quantification of gene expression with single-cell resolution overcomes these tissue-related limitations of gene expression data from pathological tissues and controls, since it enables the unbiased detection of cell-specific transcriptional dysregulation [26, 27].

Single-cell next-generation sequencing is a powerful tool to compare large numbers of single cells and to identify candidate genes, which show a dysregulated expression profile in disease conditions [28, 29]. However the large numbers of sample cells that are necessary for robust biologically meaningful results might not always be attainable. Likewise, isolated vital neurons might not be available, especially when only *post-mortem* human tissue is accessible. Therefore, the controlled isolation of desired cells with a subsequent specific analysis of identified target genes provides an alternative robust and specific experimental approach. Contact-free UV-laser microdissection (UV-LMD) is an ideal dissection method to isolate rare cell types from fixed *post-mortem* tissues (Fig. 1). In combination with reverse transcription and subsequent quantitative PCR (RT-qPCR)-based mRNA analysis of homogeneous cell pools and individual cells, provides such a candidate gene-based approach [30–37]. Here, we describe our most actual and detailed protocols for combining UV-LMD with RT-qPCR. We have specifically tailored and optimized these protocols to quantify and compare mRNA as well as miRNA levels in human SN DA neurons from *post-mortem* midbrain tissue samples of PD patients and unaffected controls, utilizing either a random primer-based reverse transcription strategy, or an oligo-dT primer-based approach, followed by qPCR (Fig. 2). Non-optimally matched samples (e.g., distinct

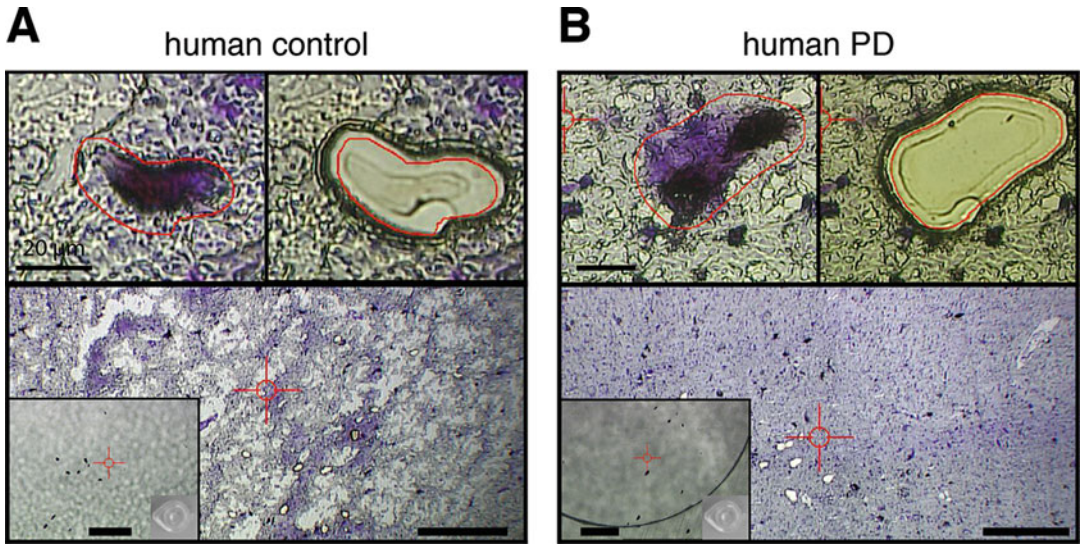


**Fig. 1** UV-laser microdissection (UV-LMD) of individual neuromelanin-positive SN DA neurons of human control (**a**) and Parkinson's disease, PD (**b**) cresylviolet-stained tissue sections. *Upper row*: individual neurons before (left) and after UV-LMD (right). Scale bars: 20 µm. *Lower row*: overview of the horizontal midbrain section containing the *Substantia nigra* after UV-LMD of 15 individual SN DA neurons. Please note the higher integrity of the PD tissue (presumably due to well-described reactive gliosis). Scale bars: 500 µm. *Inserts*: inspection of the reaction tube cap for validation of successful collection of all laser microdissected SN DA neurons. Scale bars: 400 µm

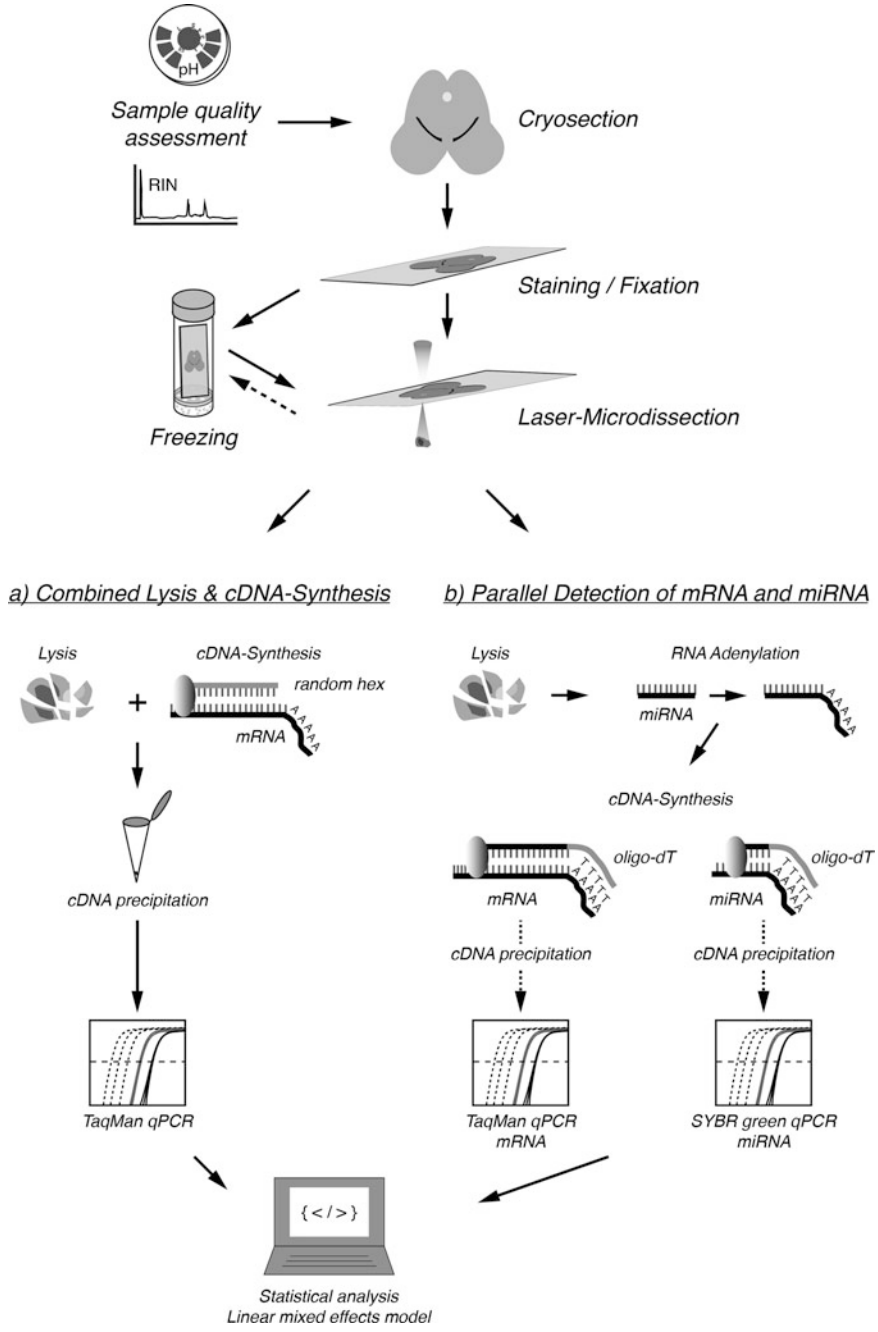


**Fig. 2** Flowchart illustrating the general experimental procedure for UV-laser microdissection (UV-LMD) and RT-qPCR-based mRNA and miRNA gene expression analysis of individual human SN DA neurons from *post-mortem* midbrains of PD patients and controls. For details, please see the text. RIN = RNA integrity number

donor ages) and different, non-optimal RNA integrities (quantified via the RNA integrity number, RIN [38]) of individual human samples are a common problem for gene expression studies of human tissue samples [39–45]. Consequently, we have not only

refined our RT-qPCR protocols, but also our data analysis, by applying an optimized linear mixed effects model to our human SN DA neuron derived UV-LMD RT-qPCR data (Fig. 2). This model allows dissecting linear contributions of distinct confounders on detected gene expression levels (i.e., distinct RINs of tissue samples, distinct ages of donors, distinct post-mortem intervals, PMIs). By comparing SN tissue-based and SN DA neuron-specific RT-qPCR results from human PD and control brains, we demonstrate that detected tissue-based gene expression differences most likely will not reflect the differential gene expression of SN DA neurons from PD and control brains [46].

With the here-detailed protocols, we identified that a variety of specific genes—coding, e.g., for ion channels, for dopamine synthesis, reuptake and packaging proteins, and for PARK gene products—display a transcriptional dysregulation in remaining human SN DA neurons from PD brains compared with those of controls [34, 37, 46–51]. These findings contribute to a better understanding of the SN DA neuron-specific pathophysiological process in PD. The identified cell-specific transcriptional dysregulations in human SN DA neurons in PD were not correlated with a respective downregulation of the miRNA miR-133b [46], as suggested by human SN tissue-based approaches [52]. We further illustrate that the application of our linear mixed effects algorithm allows further stratification of human SN DA neuron-derived RT-qPCR data, as it strongly suggests that differential gene expression of some genes (e.g., the vesicular monoamine transporter) VMAT2 is likely rather correlated with different ages of the individual analyzed human brains than with their disease state, while significantly lower mRNA levels of the transcription factor NURR1 in SN DA neurons from PD brains became evident after data stratification for distinct donor-ages and RIN of brain-samples (Fig. 3). In summary, we provide here our most actual step-by-step protocols for comparative single-cell gene expression profiling of human *post-mortem* PD and control brains, by combining UV-laser microdissection and RT-qPCR techniques that are specifically tailored for quantification of mRNA and miRNA levels in SN DA neurons from *post-mortem* human midbrains. However, most considerations and approaches are also applicable for non-candidate-gene-driven expression profiling approaches, like single-cell RNA-Seq after global RNA/cDNA amplification.

Analyzing cell-specific mRNA/miRNA levels in human *post-mortem* PD and control brains provides a particular challenge (in contrast, e.g., to analyzing perfectly matched mouse brain cohorts), due to two inevitable reasons:

1. Inevitably, the human brain samples will not be perfectly matched. Besides age, gender, and disease state, each human individual has its own genetic background and its own specific

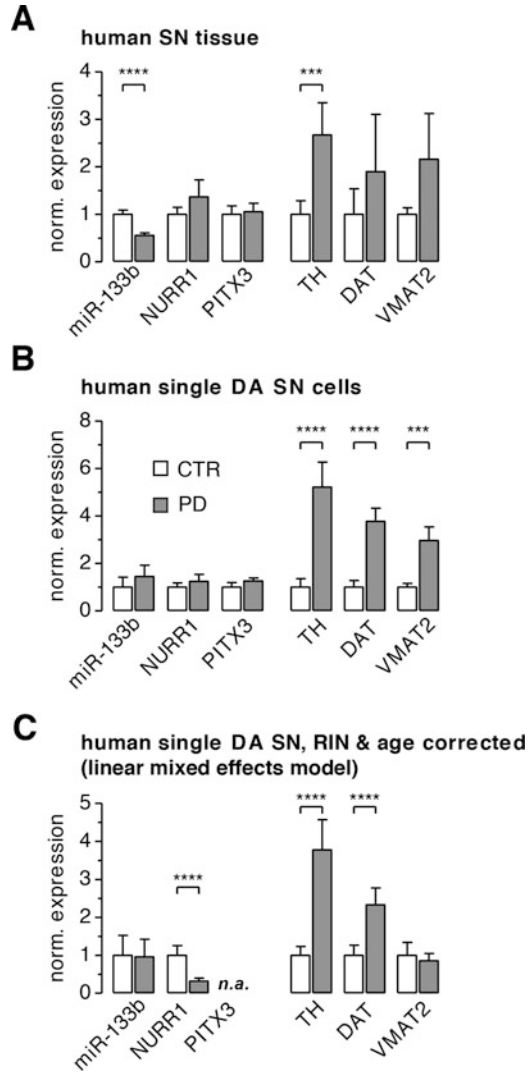


**Fig. 3** Elevated mRNA levels of dopamine release genes but not of miR-133b in SNCA-overexpressing SN DA neurons in sporadic PD. (**a**) Levels of miR-133b and mRNAs for genes involved in DA neuron development/maintenance (NURR1, PITX3) and dopamine synthesis, reuptake and vesicular packaging (TH, DAT, VMAT2), determined via RT-qPCR at the level of midbrain tissue from PD brains and controls. Tissue RT-qPCR data are normalized to a geometrical mean of β-actin, ENO2 (neuron-specific enolase) and the transcription initiation factor TIF-1A, and are given normalized to control brain levels. Note significantly lower expression of miR-133b and significantly higher levels of only TH in PD SN tissue compared to controls. (**b**/**c**) RT-qPCR analysis of genes as in (**a**), but at the cell-specific level of individual SN DA neurons, without (**b**) and after (**c**) linear mixed effects model data analysis and adjustment of data for RIN and age effects (data are given normalized to controls). (**b**) Note that miR-133b levels are not altered in SN DA neurons from PD compared to controls. These results identify the miR-133b downregulation in (**a**) and as described in [52] as a tissue-artifact, caused rather by the loss of SN DA neurons in SN-tissue in PD. These data emphasize the importance of cell-specificity when comparing gene expression in *Substantia nigra* from PD and control brains, with variations in the number of SN DA target cells due to disease state. (**c**) Note that mathematical adjustment of cell-specific data for age and RIN effects of NURR1 expression (linear mixed effects model) suggests a

life-long environmental and medical history [53–55]. Even if the provided human samples might appear well matched, they will always have a higher intrinsic heterogeneity than, e.g., respective mouse cohorts.

2. Most likely, the human brain samples will display differential degrees of RNA-degradation, depending on the circumstances of death and *post-mortem* brain removal [39–41]. In most cases, the experimenter cannot control this. It is nevertheless particularly important to avoid further degradation of RNA due to sample handling and experimental procedures.

We evolved two strategies to address these issues. First, given that our human brain samples displayed variable RIN values [56], we empirically tested that both our utilized RT-qPCR protocols were not affected by different RNA qualities, by using differently degraded RNA as RT-qPCR templates (Fig. 4). We utilized the same amounts of the same RNA as RT-qPCR templates, however with different RNA-integrities (RIN between 5.9 and 9.9, covering the range of RIN values of the human brain samples that were available to us). RT-qPCR analysis showed similar results for all the samples, unaffected by different RIN values for both RT-qPCR protocols (mouse LDH-2 assay). More importantly, both RT-qPCR protocols resulted in similar differential expression values for the PARK1/4-gene product α-synuclein for individual human SN DA neurons between PD and control brains, either if reverse transcribed with the random hexamer protocol or with the miScript oligo-dT primer-based protocol. Note that the first set of experiments and the respective third set were carried out 3 years apart (storage and re-use of human midbrain sections at −80 °C within that time). For further details *see* [46].

Second, to minimize the bias resulting from non-optimal matched tissue cohorts, we developed a model-based mathematical strategy for data analysis and stratification. After implementing a linear mixed effects model [57, 58], we dissect and subtract

**Fig. 3** (continued) downregulation of NURR1 mRNA in PD (masked by a model-suggested linear mRNA upregulation with age). Furthermore, the cell-specific elevated mRNA levels of VMAT2 in SN DA neurons in PD are not preserved after model adjustment for RIN and age effects, as VMAT2 mRNA levels of different brains are well represented by a linear age dependence, rather than by disease state. Note that model results were not reliable for PITX3 data, as the algorithm did not converge well, likely due to low numbers of samples with positive RT-qPCR results. These data highlight the power (and limitations) of the linear mixed effects model analysis of the RT-qPCR data, as the analyzed human PD and control samples were not perfectly age matched (compare Fig. 3a). Bar graphs represent normalized expression as mean ± S.E.M., asterisks indicate significant differences (***$t$-test, $p$-value $\leq$0.0001; **** $p$-value $\leq$0.00001); all data adapted from [46], for details see the text and there. *CTR* control (white bars), *PD* Parkinson's disease (grey bars), *TH* tyrosine hydroxylase, *DAT* dopamine transporter, *VMAT2* vesicular monoamine transporter 2, *ENO2* neuron specific enolase 2, *NURR1* nuclear receptor related 1 protein, *Pitx3* pituitary homeobox 3

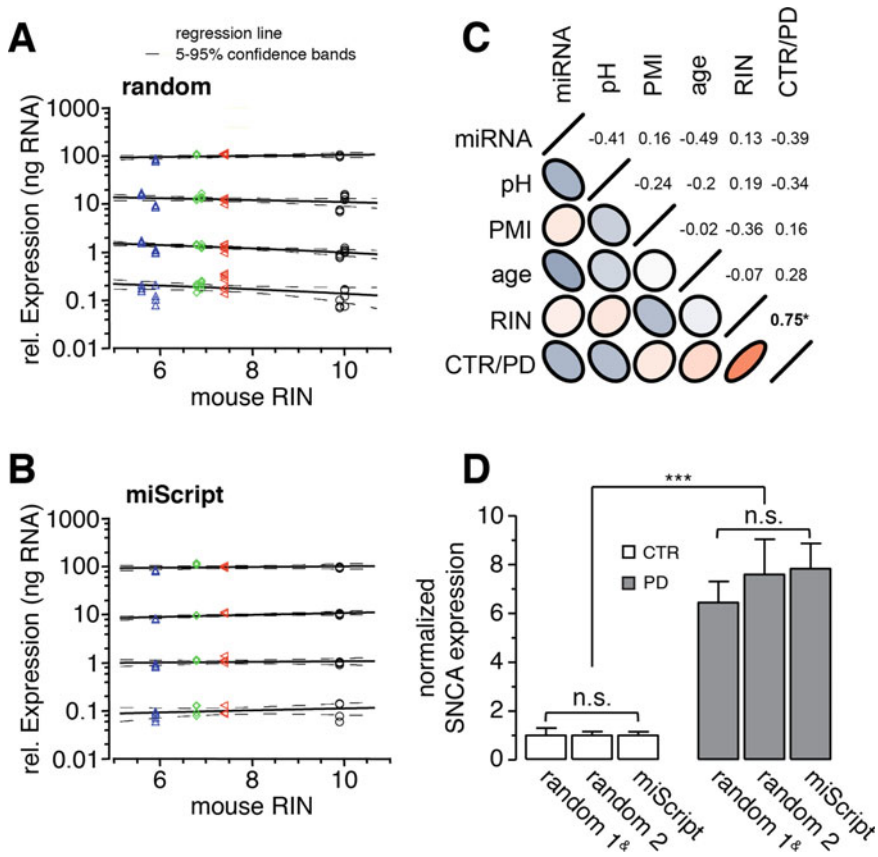


**Fig. 4** Experimental evaluation of robustness and reproducibility of two different RT-qPCR protocols for mRNA/miRNA quantification in human SN DA neurons from *post-mortem* PD and control brains. (**a**, **b**) Sensitivity and reproducibility of two different, optimized RT-qPCR protocols (**a**: random hexamer primer-based protocol; **b**: oligo-dT primer-based miScript protocol) is independent of integrity levels of RNA used as templates for cDNA synthesis (RIN range: 9.9–5.7 of mouse cDNA, covering the RIN-spectrum of the respective human samples of this study, **compare c**; qPCR assay: mLdh-2). cDNA samples with different RINs were generated by thermal degradation of the same mouse midbrain tissue derived RNA for 0–72 min at 70 °C. Results of RIN 9.9 standard curves were used for the calculation of relative expression levels of mLdh-2 at different RIN values (range: 9.9–5.9). Regression lines with confidence bands show no significant dependence of gene expression levels from RIN values at all dilutions. (**c**) Characterization and comparison of the distinct human *post-mortem* brain samples, analyzed in this study. Partial correlations between two given parameters were controlled by the other four parameters in each calculation. Shape of ellipses and color define strength of correlation (red: positive correlation, right leaning ellipse; blue: negative correlation, left leaning ellipse). Asterisk indicates significance; $p = 0.75$. Note the particularly strong and significant correlation between RNA quality (given as RNA integrity number RIN) and disease state (control CTR vs. Parkinson's disease, PD), due to significant difference of RIN values between control brains (CTR, $n = 8$) and PD brains ($n = 5$). *RIN* RNA integrity number, *PMI post-mortem* interval, *miRNA* microRNA. (**d**) Using the oligo-dT primer-based miScript RT-qPCR protocol, similar degrees of significantly elevated alpha-synuclein (SNCA) mRNA levels were detected in remaining human SN DA neurons from PD brains compared to those of controls, as with the random hexamer based RT-qPCR protocol. Random 1 data adapted from [48], random 2 as well as miScript data adapted from [46], for details see the text and there. Bar graphs (mean ± S.E.M.) show normalized SNCA expression levels of three individual human SN DA sample sets from control brains (random 1, miScript 5: $n = 5$ brains; random 2: $n = 8$ brains) and PD brains ($n = 5$). Asterisks (***) indicate significant difference (*t*-test, *p*-value $\leq 0.0001$)

possible linear influences of distinct confounders on RT-qPCR data—in our case distinct age—and RIN-values of individual brains, but the model is also applicable, e.g., to distinct *post-mortem* intervals (PMI) or tissue pH-values [46, 59].

## 2 Materials

### 2.1 Handling, Fixation, and Staining of Human Brain Tissue

1. To prevent RNase contamination, human brain tissue specimens are stored in heat-sterilized tinfoil and RNase-ExitusPlus (AppliChem) treated parafilm-sealed boxes at −80 °C.
2. Molecular biology grade, certified RNase-free $H_2O$ and ethanol are used. Primer/reagent solutions as well as mastermixes are prepared with RNase-free $H_2O$ supplied by 5 PRIME.
3. Microtome blades (Feather, Type R35) are rinsed two times for 30 s in 75% ethanol and whipped with RNase-ExitusPlus and RNAse-free isopropanol (Sigma) (*see* **Note 1**).
4. Ethanol dilution series (2× 75%, 95%, 100% absolute (Sigma) and one tube Ethanol anhydrous (Alfa Aesar, see below)) are freshly prepared with RNAse-free $H_2O$ (Qiagen) on each experimental day and stored in 50 ml Falcon tubes at room temperature. One tube of 75% ethanol is kept at −20 °C. Ethanol anhydrous stock (90% ethanol, 5% methanol, 5% isopropanol, AlfaAesar) is stored with molecular sieve (Merck, pore size: 0.3 nm, 25 g/l) to avoid rehydration.
5. 1% Cresyl Violet (CV) acetate staining dye (Sigma) is diluted in 100% ethanol (Sigma), stored in a tinfoil covered and parafilm sealed Falcon tube, and incubated for at least 1 week before use, as CV dissolves non-optimal in ethanol.
6. A RNase-free drying box with Silica gel with moisture indicator (Merck) is used.
7. pH values of human *post-mortem* midbrain tissue samples are analyzed with a pH Optica micro system and a pH MicroTip Fiber Optic sensor, 140 μm OD (both WPI).
8. RNA integrity number (RIN) analysis, a measure for RNA degradation [56], is performed with the Agilent 2100 Bioanalyzer system. For mRNA integrity analysis the Agilent RNA 6000 Nano Chip Kit, and for analysis of small RNA amounts and % miRNAs the Agilent Small RNA Chip-Kit are used.

### 2.2 UV-Laser Microdissection

1. A contact-free UV-laser microdissection (UV-LMD) microscope is needed (this protocol was successfully tested with both, the Zeiss PALM UV-LMD setup and the Leica UV-LMD6000 and UV-LMD7000 setups; currently we only use the UV-LMD7000). Heat-sterilization (180 °C, 2 h) of all UV-LMD microscope parts that are in contact with the tissue

slides (i.e., slide holder) or reaction tubes (i.e., cap/tube holder, forceps) prevents RNase contamination (*see* **Note 1**).

2. PEN-membrane slides (MicroDissect, 2.0 μm) for mounting of tissue sections and laser microdissection are treated with UV-C light for 20 min.
3. RNase-free thin-walled 0.5 ml PCR reaction tubes with flat cap (Axygen PCR thin-wall, clear, 0.5 ml) are UV-C treated with an open cap for 45 min, before using them for cell collection, combined cell lysis and cDNA synthesis, and cDNA precipitation.

### 2.3 Cell-Lysis and Reverse Transcription

#### 2.3.1 Preparation of Cap-Mix for Combined Cell Lysis and cDNA Synthesis

1. Cell lysis and cDNA synthesis are performed in the same buffer (*Cap-Mix*) containing 0.5% NP-40 (Roche, light sensitive, stored as 10% stock in aliquots in the dark at +4 °C), 5 U SUPERase-In (Thermo Fisher Scientific, stored in aliquots at −20 °C), 0.5 mM dNTPs (GE Healthcare, stored as 20 mM stock at −20 °C), 5 μM random hexamer primers (Roche, stored as 1 mM stock aliquots at −20 °C), 500 ng poly-inosine (Sigma, stored as 1 μg/μl stock at −20 °C), 2 mM Tris-HCl pH 7.4 (Sigma, 100 mM stock stored at −20 °C), 10 mM DTT (Thermo Fisher Scientific, stored as 100 mM stock at −20 °C) in 1× first-strand buffer (Thermo Fisher Scientific, 5× stock: 250 mM Tris-HCl, 375 mM KCl, 15 mM $MgCl_2$, pH 8.3, stored in aliquots at −20 °C) at a final volume of 4.7 μl per reaction.
2. *Cap-Mix* sufficient for the number of samples that are collected (plus positive and negative controls) is freshly prepared on each experimental day (*see* **Note 2**) and stored on ice in a light-protected, RNase-free 0.5 ml single sealed reaction tube (Eppendorf biopure, tube shaft and lid covered with tube labels). All the components are carefully added, mixed by finger flipping and quickly centrifuged. SUPERase-In is added directly from −20 °C to the reaction mix. Poly-inosine, NP-40, and SUPERase-In are viscous and special care has to be taken during pipetting to avoid air bubbles or volume errors. If bubbles have formed, the mix is centrifuged briefly until all bubbles disappear (*see* **Notes 3** and **4**).
3. 60 U (=0.3 μl) SuperScript II Reverse Transcriptase (Thermo Fisher Scientific, stored in aliquots at −20 °C) are added to each reaction after lysis (*see* Subheading 3.3). The enzyme aliquots are stored in a benchtop freezer (Techne) at −20 °C during the experiment to avoid "freeze-thaw-cycles."

#### 2.3.2 Preparation of Lysis Mix and miScript Buffer Mix for Cell Lysis with Subsequent miScript Reverse Transcription

1. Cell lysis is performed in the *miRNA lysis mix* containing 0.5% NP-40 (Roche, light sensitive, stored as 10% stock in aliquots in the dark at +4 °C; final concentration after reverse transcription 0.25%), 10 U SUPERase-In (Thermo Fisher Scientific, stored in aliquots at −20 °C), 500 ng poly-inosine (Sigma, stored as 1 μg/μl stock at −20 °C) at a final volume of 5 μl per reaction.
2. miRNA lysis mix sufficient for the number of samples that are collected (plus positive and negative controls) is freshly prepared on each experimental day as described above.
3. Parallel reverse transcription of mRNA and miRNA is performed by adding 4.5 μl of the *miScript buffer mix* (2 μl 5× *miScript RT buffer*, miScript Reverse Transcription Kit, Qiagen, and 2.5 μl RNase-free $H_2O$ (5 PRIME)) and by the addition of 0.5 μl *miScript RT mix* (containing polyadenylase and reverse transcriptase, miScript Reverse Transcription Kit, Qiagen) in a final volume of 10 μl per reaction.

### 2.4 cDNA Precipitation

Depending on the subsequent processing of the cDNA, a purification step via ethanol precipitation is recommended [60].

1. cDNA precipitation should be performed in a reaction tube, which is suited for longer high-speed centrifugation. As cDNA precipitation of UV-LMD samples should best be performed in the same tube after reverse transcription, employing a reaction tube that is tested and established for both, UV-LMD and cDNA precipitation is strongly recommended.
2. cDNA precipitation is performed with *precipitation-mix* containing 1 μg glycogen (stored as 1 μg/μl stock-solution at −20°C, Thermo Fisher Scientific), 350 ng PolydC (stored as 1 μg/μl stock-solution at −20°C, Midland) and 1/10 volume sodium acetate (NaAc, i.e., 1.2 μl of 3 M stock-solution, pH 5.5, stored at room temperature, Thermo Fisher Scientific) added to 4.8 μl $H_2O$ (5 PRIME) in a total volume of 7.3 μl.
3. cDNA *precipitation mix*, sufficient for the number of samples, plus positive and negative controls is freshly prepared on each experimental day. All the components are carefully added, mixed by vortexing, and quickly centrifuged. As precipitation control, serial cDNA dilutions for generation of a qPCR standard curve are precipitated and analyzed in respect to the respective non-precipitated cDNA standard curve.
4. Certified RNase-free ethanol is used for cDNA precipitation.

### 2.5 Quantitative Real-Time PCR

1. cDNA for the generation of standard curves (serial dilutions over four magnitudes, e.g., 30–0.03 ng) to assess assay performance is needed, e.g., human tissue SN cDNA (1 μg/μl,

derived from Human Brain, Substantia Nigra Total RNA, Clontech/TaKaRa).

2. A GeneAmp 7900HT real-time qPCR system (Applied Biosystems) or comparable instrument and 96-well PCR plates (Thermo Fisher Scientific) with optical adhesive film covers (Thermo Fisher Scientific) are needed.

*2.5.1 TaqMan PCR Reaction Contents*

1. 2× QuantiTect Probe qPCR Master Mix (Qiagen).
2. 20× TaqMan PrimerProbe Assay (Life Technologies, for details *see* **Notes 5** and **10**).

*2.5.2 SYBRgreen PCR Reaction Contents (for miRNA Amplification)*

1. 2× QuantiTect SBYR Green PCR Master Mix (Qiagen).
2. 10× miScript Universal Primer (sequence: company properties, Qiagen).
3. 10× miScript Assay (in 1× Tris-EDTA, pH 8, Qiagen, *see* **Note 10**).

### 2.6 Linear Mixed Effects Model

1. R project software for statistical computing (R-Development-Core-Team, 2012), Version 2.15.1 or later.
2. R-package ASReml-R (VTN International Ltd., Hemel Hempstead, UK).

## 3 Methods

To guarantee successful UV-LMD and subsequent gene expression analysis of small cell pools and individual cells, it is essential to work in a strictly RNase-free regime. For details on RNase-free working conditions, *see* **Note 1**. The protocol described below was used to quantify mRNA/miRNA levels in neuromelanin-positive SN DA neurons from human *post-mortem* midbrain tissue blocks, provided by the German BrainBank. An overview of the experimental procedures is illustrated in Fig. 1.

### 3.1 Storage, Cryosectioning, and Staining of Human Brain Tissue

1. On the experimental day, human brain tissue is transferred (on dry ice) from −80 °C to the quick-freeze panel of a precooled cryostat (−35 °C) and glued with tissue freezing medium (Leica) on a specimen holder (*see* **Note 6**). After an equilibration period of 20 min at −35 °C, the cryostat is set to the cutting temperature (for our specimens −19 °C), and additionally equilibrated for 45 min, before 12 μm horizontal midbrain sections including the SN are cut. Chippings from the trimming procedure are collected for RNA quality and tissue pH analysis (*see* Fig. 1 and **Note 7**).
2. The brain sections are mounted on UV-C treated PEN-membrane slides and allowed to thaw briefly. Once thawed, the slide is transferred to the Falcon tube with 75% ethanol at −20 °C and fixed for 2 min.

3. The slide is removed with a sterile forceps, and 0.25 ml 1% cresyl violet staining solution is applied directly on the slide via a sterile filter syringe (0.1 μm; Whatman), incubated for 1 min, then dipped briefly in 75%, 95% and 100% ethanol absolute and finally incubated for 1 min in ethanol anhydrous.
4. The fixed and stained slides, each containing several brain sections, are stored in a drying chamber containing silica gel for at least 45 min before UV-LMD.
5. Alternatively, after drying, the slides are long-term stored at −80 °C in storage jars, containing silica gel (*see* Fig. 1 and **Note 8**).
6. For human brain pH value analysis, tissue chippings (*see* **Note 7**) are homogenized in 4 °C cold $H_2O$ (10 μl per mg tissue) with a sterile 1 ml syringe and a 21-gauge needle. The MicroTip fiber optic pH sensor is calibrated at 4 °C. Measurements are performed on ice or room temperature.
7. RIN values as well as amounts of small RNAs and % of miRNA are determined from RNA, isolated from human brain tissue chippings (*see* Fig. 1 and **Note 7**) via the RNeasy MINI kit (Qiagen), eluted in an volume of 30 μl $H_2O$ (5 PRIME). 1.5 μl of eluted RNA is mixed with 5 μl of fluorescence marker and run on an Agilent RNA 6000 Nano Chip or the Agilent Small RNA Chip, respectively.

### 3.2 UV-Laser Microdissection of Individual Neurons from Human Brain Samples

1. All workspaces are cleaned to ensure RNase-free working conditions (*see* **Note 1**).
2. Slides with tissue sections are placed on the sterile slide holder and transferred to the UV-LMD microscope. Tissue quality and staining are inspected under low and high magnifications, and only sections that allow clear identification of individual cells are further processed (*see* Fig. 2). For the identification of individual human SN DA neurons, their brown-black neuromelanin content is very helpful.
3. Laser-settings need to be optimized for each individual section.
4. After the brain region of interest is identified (in our case SN), an UV-C treated thin-walled PCR reaction tube is placed in the cap holder and transferred to the microscope. The reaction tube cap is inspected with the *cap-control* function to exclude rarely occurring contaminations with dust particles. Individual SN DA neurons are cut and harvested into the cap of the reaction tube. It is highly recommended to visually control that all laser microdissected neurons were successfully harvested (*cap-control* function, *see* Fig. 2).

### 3.3 Lysis and cDNA Synthesis of Individual Laser Microdissected Neurons from Human Brain Samples with Random Hexamer Primers

For each set of single-cell experiments, suitable positive controls (e.g., cDNA; derived from commercially obtained human SN tissue RNA, *see* Subheading 2.5.1) and negative controls (no UV-LMD harvested cells in cap) are processed in parallel.

1. If the *cap-control* is positive, the cap holder is removed and 4.7 μl *Cap-Mix* are added to the cap immediately. Any direct contact between the cap and the pipette tip must be avoided.
2. The reaction tube is carefully removed from the cap holder and the tube is closed upside down to ensure that the *Cap-Mix* remains in the cap.
3. The reaction tube is placed upside down on the cap in a preheated (72 °C) thermoblock (ThermoStat, Eppendorf) and incubated for 2 min for cell lysis (*see* **Note 9**).
4. Afterwards the tube is transferred onto an ice-cold metal block, upside-down, and allowed to cool for 5 s.
5. The *Cap-Mix* is then spun down at 11,200 × *g* with a benchtop centrifuge (MiniSpin plus, Eppendorf) for 1 min at room temperature and transferred onto an ice-cold metal block to cool down for 1 min.
6. 0.3 μl SuperScript II are added directly to the *Cap-Mix* in the bottom of the tube.
7. The tube is transferred to a preheated (38 °C) thermomixer (Eppendorf, 350 rpm for 10 s every 10 min) and random hexamer-based cDNA synthesis is carried out overnight. For overnight incubation, after 2 h at 38 °C, all the samples are spun down briefly, and are transferred to a preheated thermobox (ThermoStat, Eppendorf) for final overnight cDNA synthesis (39 °C). After cDNA synthesis, the samples are stored at −20 °C until further processing.

### 3.4 Combined Lysis and cDNA Synthesis with Oligo-dT-Primers (miScript)

1. If the *cap-control* is positive, the cap holder is removed and 5 μl *miRNA lysis Mix* is added to the cap immediately. Any direct contact between the cap and the pipette tip must be avoided.
2. The reaction tube is carefully removed from the cap holder and the tube is closed upside down to ensure that the *miRNA lysis Mix* remains in the cap.
3. The reaction tube is placed upside down on the cap in a preheated (72 °C) thermobox (ThermoStat, Eppendorf), and incubated for 2 min for cell lysis (*see* **Note 9**).
4. Afterwards the tube is transferred onto an ice-cold metal block, upside-down, and allowed to cool for 1 min.
5. The *miRNA lysis Mix* is then spun down at 11,200 × *g* with a benchtop centrifuge (MiniSpin plus, Eppendorf) for 1 min at room temperature.

6. 4.5 µl *miScript buffer mix* and 0.5 µl *miScript RT mix* are added directly to the *miRNA lysis Mix* in the bottom of the tube after spinning.
7. The tube is transferred to a preheated (38 °C) thermomixer (Eppendorf, 350 rpm for 10 s every 10 min) and polyadenylation and cDNA synthesis are carried out for at least 2 h or overnight. After cDNA synthesis, the samples are stored at −20 °C until further processing.

### 3.5 cDNA Precipitation

1. 7.3 µl of the *precipitation-mix* are added directly to each 5 µl cDNA reaction into the cDNA reaction tube. The samples are vortexed thoroughly and briefly centrifuged.
2. About 3 volumes of 100% ethanol (40 µl, Applichem) are added. The samples are vortexed thoroughly and briefly centrifuged.
3. The samples are precipitated overnight at −20 °C.
4. Reaction tubes are centrifuged at 0 °C at 16,100 rcf for 2 h.
5. The supernatant of each sample is discarded via pipetting. Physical contact with the cDNA pellet is carefully avoided.
6. 100 µl of 80% ethanol (Applichem) are added (pellet should not be resuspended or vortexed), the samples are centrifuged for 15 min at 0 °C and the supernatant is again carefully discarded via pipetting.
7. cDNA pellets are dried in opened reaction tubes at 45 °C for 10 min in a ThermoMixer (Eppendorf).
8. The desired volume of $H_2O$ (5 PRIME) is added. Contact of the cDNA pellet with the pipet tip is avoided. Tubes are closed, shortly centrifuged and incubated for 2 h at 45 °C in a ThermoMixer (Eppendorf) with interval shaking (550 rpm for 10 s every 10 min) to dissolve cDNA pellets. Samples are spun down at least each 40 min (three times).

### 3.6 Quantitative Real-Time PCR of UV-LMD cDNA Samples for mRNA and miRNA Quantification

1. The following procedures are carried out in a UV-C treated sterile workbench.
2. Best, precipitated cDNA is used (*see* Subheading 3.4). If cDNA is NOT precipitated, it has to be diluted at least tenfold to avoid inhibitory effects of the RT-reaction on the qPCR [60]. In this case, each single-cell cDNA sample is diluted by adding 50 µl (random hexamer samples) or 45 µl (miScript samples) molecular biology grade $H_2O$ (5 PRIME).
3. Tubes are stored in ice-cold metal blocks.
4. A serial dilution of a cDNA standard (see above Subheading 2.5.1) is run in parallel with each experiment (*see* Subheading 2.5), as a PCR positive control, and for standard curve generation to assess assay performance and to calculate the cDNA amount of the UV-LMD samples in respect to the standard curve.

### 3.7 TaqMan PCR (for mRNA qPCR Amplification)

1. A mastermix for each individual gene of interest for all the samples for quantitative real-time PCR in 20 µl reactions is prepared by mixing 10 µl 2× QuantiTect Probe qPCR Master Mix, 1 µl 20× primer/probe mix (for gene of interest, for details **Notes 5** and **10**) and 4 µl $H_2O$ (depending on the cDNA volume used) for each UV-LMD sample (volumes are multiplied by the number of samples + controls + 1).
2. 15 µl of respective mastermix is added to the bottom of a MicroAmp 96-well reaction plate. 5 µl of cDNA (adjust volumes accordingly if cDNA in more or less volume is used) is added to the mastermix and the plate is sealed with an *optical adhesive cover*. After 2 min centrifugation (1027 rcf, at 4 °C) the plate is transferred to a real-time PCR system (e.g., HT7900, Applied Biosystems) and the qPCR reaction is run using the following cycling conditions (specific for our TaqMan assays): 2 min at 50 °C, 15 min at 95 °C, and subsequently 50 cycles of 0:15 min at 94 °C and 1 min at 60 °C each.

### 3.8 SYBRgreen PCR (for miRNA qPCR Amplification)

1. A mastermix for each individual gene of interest for all samples for quantitative real-time PCR in 25 µl reactions is prepared by mixing 12.5 µl 2× QuantiTect SYBRgreen qPCR Master Mix, 2.5 µl 10× miScript Universal primer mix, 2.5 µl 10× miScript primer assay (for gene of interest, e.g., miR-133b, for details **Note 10**) and 2.5 µl $H_2O$ for each UV-LMD sample/PCR-reaction (volumes are multiplied by the number of samples + controls + 1).
2. 20 µl of mastermix is added to the bottom of a MicroAmp 96-well reaction plate. 5 µl of cDNA (adjust volumes accordingly if cDNA in more or less volume is used) is added to the mastermix and the plate is sealed with an optical adhesive film. After 2 min centrifugation (1027 rcf, at 4 °C) the plate is transferred to a real-time PCR system (i.e., HT7900, Applied Biosystems) and the qPCR reaction is run using the following cycling conditions (specific for miScript assays, Qiagen): 15 min at 95 °C and subsequently 50 cycles, 0:15 min at 94 °C, 0:30 min at 55 °C, 0:30 min at 70 °C, and 0:30 min at 73 °C (fourth segment), followed by a melting curve (0:15 min at 95 °C, 0:15 min at 60 °C, subsequent continuous increase of 1 °C every 0:15 min under the detection of the fluorescence signal up to 95 °C).

### 3.9 Data Analysis

1. For SYBRgreen PCR, the first step is a melting curve analysis, to ensure PCR-product specificity, as well as correct read-out temperature (fourth segment). Afterwards, data analysis of TaqMan as well as of SyberGreen qPCR are identical.
2. Fluorescence amplification plots are analyzed first without normalization to the internal fluorescence standard dye ROX (carboxy-X-rhodamine, as passive reference dye), to evaluate

absolute fluorescence signals, background noise levels, and possible confounders.

3. TaqMan probe or SYBRgreen fluorescence signals are normalized to the ROX-signals, and the baseline for normalization is set (usually cycles 3–15).
4. It must be ensured that all negative controls did not result in any detectable qPCR signal.
5. The detection threshold is set in the exponential phase of the qPCR amplification plot (illustrated in Fig. 1). To quantify the expression of a respective gene via qPCR for a set of samples, the same threshold value is used for all the samples and for the standards (run in parallel). *Threshold cycle* ($C_t$) values of each sample as well as slope and $\Upsilon$-intercept of the standard curve can be read out from the sequence detection software (e.g., SDS2.4, Applied Biosystems).
6. The average cDNA amount per cell in relation to the utilized cDNA standard curve is calculated according to:

$$\text{cDNA amount per cell} = \frac{S^{\left[\left(C_t - \Upsilon_{\text{intercept}}\right)/\text{slope}\right]}}{\text{No}_{\text{cells}} \bullet \text{cDNA fraction}}$$

*S* corresponds to the serial dilution factor of the standard curve (e.g., 10 for serial dilution in steps of 10), $\text{No}_{\text{cells}}$ to the number of harvested neurons per sample and cDNA fraction to the fraction of the UV-LMD cDNA sample used as template in the real-time PCR reaction, e.g., 5/55. The unit-magnitude corresponds to the respective standard utilized, which defines the unit at the $\Upsilon_{\text{intercept}}$ (e.g., pg-equivalents of standard cDNA, derived from SN-tissue/cell). For better comparison, expression data can be further normalized to those of control brains (mean controls = 1; compare Figs. 3 and 4d). Alternatively, an absolute standard curve with quantified numbers of RNA or cDNA molecules as templates can be generated, and data are analyzed as described above [61, 62].

### 3.10 Linear Mixed Effects Model

RT-qPCR data can be further analyzed and corrected for confounding effects, like distinct RINs and ages of human brains, by applying a linear mixed effects model (Figs. 3c and 4c). Our modeling approach assumes a log-linear dependency of RT-qPCR data from age- and RNA-values. Since this is likely to be a simplification, it is mandatory to analyze the goodness-of-fit and applicability of the modeling approach (e.g., $R^2$ values, proportional change in variance, PCV, and Bayesian information criterion, BIC; for details *see* [46] supplementary material).

Fitting and correction for confounding variables (like age- and RIN-values) and subsequent statistical analysis of adjusted data is carried out on log-transformed expression data, which show a more

symmetric distribution closer to Gaussian. Back-transformation of adjusted data is then done on this assumption of a log-normal distribution. Uncertainties of the regression are considered in the standard errors of means by applying rules of uncertainty and error propagation [63]. From the resulting parameter values (in log-transformed scale) differences in mRNA-levels between control and PD groups are tested for statistical significance by Student's *t*-test (Welch-Test). The general model-based analysis procedure is as follows:

1. Logarithmic transformation of RT-qPCR data.

$$f : \log\aleph(E, \mathrm{Var}) \rightarrow \aleph\left(\mu, \sigma^2\right) \text{ defined by } f\left(\boldsymbol{Y}_{i,j}\right) := \ln \boldsymbol{Y}_{i,j}$$

$\aleph$: normal distribution
$\boldsymbol{Y}_{i,j}$: data vector of measured values for gene $i$ and brain $j$
$E$, $Var$: mean and variance of data (original scale)
$\mu$,$\sigma^2$: mean and variance of log-transformed data

2. Fitting of the linear mixed effects model with ASReml-R.

$$\ln \boldsymbol{Y}_{i,j} = \beta_i^{\mathrm{C/PD}} x_j^{\mathrm{C/PD}} + \beta_i^{\mathrm{age}} x_j^{\mathrm{age}} + b_i^{\mathrm{RIN}} x_j^{\mathrm{RIN}} + \left(\beta_i^0 + \gamma_{i,j}^0\right) + \boldsymbol{e}_{i,j}$$

$$b_i^{\mathrm{RIN}} = \beta^{\mathrm{RIN}} + \gamma_i^{\mathrm{RIN}}$$

$\boldsymbol{Y}_{i,j}$: data vector of measured values for gene $i$ and brain $j$
$\beta_i^{\mathrm{C/PD}}, \beta_i^{\mathrm{age}}, \beta^{\mathrm{RIN}}$: fixed effects for group (control or PD), age and RIN of gene $i$
$\beta_i^0, \gamma_{i,j}^0$: intercept of gene $i$ and its random contribution for brain $j$
$\gamma_i^{\mathrm{RIN}}$: random effect for RIN dependence of gene $i$
$b_i^{\mathrm{RIN}}$: total RIN dependence of gene $i$
$\boldsymbol{e}_{i,j}$: residuals (fitted values−mesured values) of each individual gene $i$ and brain $j$
$x_j^{\mathrm{C/PD}}, x_j^{\mathrm{age}}, x_j^{\mathrm{RIN}}$: group (control, PD), age and RIN value of brain $j$
(independent variables $y = f(x)$)

3. Adjustment of each RT-qPCR value for confounders (age, RIN).

$$\ln \tilde{\boldsymbol{Y}}_{i,j} = \ln \boldsymbol{Y}_{i,j} + \beta_i^{\mathrm{age}} \Delta x_j^{\mathrm{age}} + \left(\beta^{\mathrm{RIN}} + \gamma_i^{\mathrm{RIN}}\right) \Delta x_j^{\mathrm{RIN}} + \boldsymbol{e}_{i,j}$$

$$\text{with } \Delta x_j^{\mathrm{age}} = \bar{x}_{\mathrm{age}} - x_j^{\mathrm{age}} \text{ and } \Delta x_j^{\mathrm{RIN}} = \bar{x}_{\mathrm{RIN}} - x_j^{\mathrm{RIN}}$$

$\tilde{\boldsymbol{Y}}_{i,j}$ : RIN and age adjusted expression values for gene $i$ and brain $j$

$\boldsymbol{\Upsilon}_{i,j}$: data vector of measured values for gene $i$ and brain $j$
$\beta_i^{\mathrm{C/PD}}, \beta_i^{\mathrm{age}}, \beta^{\mathrm{RIN}}$: fixed effects for group (control or PD), age and RIN of gene $i$
$\bar{x}_{\mathrm{age}}$: mean of age values
$\bar{x}_{\mathrm{RIN}}$: mean of RIN values
$x_j^{\mathrm{C/PD}}, x_j^{\mathrm{age}}, x_j^{\mathrm{RIN}}$: group membership (control or PD), age and RIN value of brain $j$
$\gamma_i^{\mathrm{RIN}}$: random effect for RIN dependence of gene $i$
$\boldsymbol{e}_{i,j}$: residuals on single sample level for each gene $i$ and brain $j$

4. Computation of standard errors for each brain's expression values by applying rules of uncertainty propagation.

$$\theta_{i,j} = \sqrt{\left(\sigma_i^{\mathrm{age}} \Delta x_j^{\mathrm{age}}\right)^2 + \left(\sigma_i^{\mathrm{RIN}} \Delta x_j^{\mathrm{RIN}}\right)^2}$$

with $\Delta x_j^{\mathrm{age}} = \bar{x}_{\mathrm{age}} - x_j^{\mathrm{age}}$ and $\Delta x_j^{\mathrm{RIN}} = \bar{x}_{\mathrm{RIN}} - x_j^{\mathrm{RIN}}$

$\theta_{i,j}$: standard error of adjustment
$\sigma_i^{\mathrm{age}}$: standard error of age effect $\beta_i^{\mathrm{age}}$ for gene $i$
$\sigma_i^{\mathrm{RIN}}$: standard error of RIN effect $\left(\beta^{\mathrm{RIN}} + \gamma_i^{\mathrm{RIN}}\right)$ for gene $i$

5. Determination of parameters (mean and standard errors) of normal distributions of adjusted values and their adjusted errors.

$$\widetilde{\mu}_{i,k} = \frac{\sum \tilde{\boldsymbol{Y}}_{i,j}}{N_{i,k}}, \quad \widetilde{\sigma}_{i,k}^2 = \mathrm{Var}\left(\tilde{\boldsymbol{Y}}_{i,j}\right) + \frac{\sum \left(\theta_{i,j}\right)^2}{N_{i,k}}$$

for data of brains $j$ belonging to group $k \epsilon \{\mathrm{C}, \mathrm{PD}\}$
$\tilde{\boldsymbol{Y}}_{i,j}$ : RIN and age -adjusted expression values for gene $i$ and brain $j$
$\widetilde{\mu}_{i,k}$ : mean of adjusted log-transformed expression values in group $k$ gene $i$
$\widetilde{\sigma}_{i,k}^2$: variance of adjusted log-transformed expression values in group $k$ for gene $i$
$N_{i,k}$: number of observations in group $k$ for gene $i$
Var(): variance of data
$\theta_{i,j}$: standard error of adjustment

6. Test for differences between control and PD groups by applying Student's $t$-test (Welch-Test).

$$t\text{-test statistic} : t = \frac{\widetilde{\mu}_{i,\mathrm{PD}} - \widetilde{\mu}_{i,\mathrm{C}}}{\sqrt{\widetilde{\mathrm{se}}_{i,\mathrm{PD}}{}^2 + \widetilde{\mathrm{se}}_{i,\mathrm{C}}{}^2}}$$

$$\text{and degrees of freedom : df} = \frac{\left(\widetilde{\text{se}}_{i,\text{PD}}{}^2 + \widetilde{\text{se}}_{i,\text{C}}{}^2\right)^2}{\frac{\widetilde{\text{se}}_{i,\text{PD}}{}^2}{N_{i,\text{PD}}-1} + \frac{\widetilde{\text{se}}_{i,\text{C}}{}^2}{N_{i,\text{C}}-1}}$$

with squared standard error of means:

$$\widetilde{\text{se}}_{i,\text{PD}}{}^2 = \widetilde{\sigma}^2_{i,\text{PD}}/N_{i,\text{PD}} \text{ and } \widetilde{\text{se}}_{i,\text{C}}{}^2 = \widetilde{\sigma}^2_{i,\text{C}}/N_{i,\text{C}}$$

$\widetilde{\mu}_{i,\text{C/PD}}$: mean of adjusted log-transformed expression values for gene $i$ from C or PD
$\widetilde{\sigma}^2_{i,\text{C/PD}}$: variance of adjusted log-transformed expression values for gene $i$ in C or PD
$N_{i,\text{C/PD}}$: number of observations for gene $i$ in C or PD group

7. Back-transformation from log-transformed to original scale by the computation of mean values and variances from parameter values of normal distributions in the transformed space.

$$\tilde{E}_{i,k} = e^{\widetilde{\mu}_{i,k}+\widetilde{\sigma}^2_{i,k}/2}, \qquad \widetilde{\text{Var}}_{i,k} = \left(e^{\widetilde{\sigma}^2_{i,k}} - 1\right) e^{2\widetilde{\mu}_{i,k}+\widetilde{\sigma}^2_{i,k}}$$

with $k\epsilon\{\text{C, PD}\}$
$\tilde{E}_{i,k}$: mean of adjusted data in original scale (pg cDNA/cell)
$\widetilde{\mu}_{i,k}$ : mean of adjusted log-transformed expression values in group $k$ for gene $i$
$\widetilde{\sigma}^2_{i,k}$: variance of adjusted log-transformed expression values in group $k$ for gene $i$
$\widetilde{\text{Var}}_{i,k}$: variance of adjusted data in original scale

8. To assess goodness-of-fit, $R^2$ values as well as *proportional change in variance* (PCV) are determined at the brain level, as suggested in [58, 64].

$$R^2_i = 1 - \frac{\text{MSPE}_i}{\text{MSPE}_{0,i}} \text{ with mean squared prediction error MSPE}_i$$
$$= \frac{\text{Var}(\boldsymbol{e}_i)}{n_i} + \text{Var}\left(\boldsymbol{\gamma}^0_{\boldsymbol{i}}\right)$$

$\text{MSPE}_{0,i}$: MSPE of a reference model, e.g., the empty model of gene $i$
Var ($\boldsymbol{e}_i$): variance of residuals for gene $i$
$n_i$: number of samples from each brain for gene $i$ ($n_i$=10)
$\text{Var}\left(\boldsymbol{\gamma}^0_{\boldsymbol{i}}\right)$: variance of random effects for gene $i$

and

$$R^2_{\text{marg},i} = \frac{\sigma_f^2}{\sigma_f^2 + \text{Var}\left(\gamma_i^0\right) + \text{Var}(\boldsymbol{e_i})}, \quad R^2_{\text{cond},i} = \frac{\sigma_f^2 + \text{Var}\left(\gamma_i^0\right)}{\sigma_f^2 + \text{Var}\left(\gamma_i^0\right) + \text{Var}(\boldsymbol{e_i})}$$

$R^2_{\text{marg},i}$: marginal $R^2$, variance explained by fixed effects only.
$R^2_{\text{cond},i}$: conditional $R^2$, variance explained by fixed and random effects.
$\sigma^2_{f,i}$: variance calculated from the fixed effect components of the mixed effects model.

and PCV:

$$\text{PCV}_i = 1 - \frac{\text{Var}\left(\gamma_i^0\right)}{\text{Var}\left(\gamma^0_{\text{ref},i}\right)}$$

$\text{Var}\left(\gamma^0_{\text{ref},i}\right)$: variance of random effects of reference model, e.g., the empty model.

9. In addition, a relative adjustment error can be computed as

$$\varepsilon_i = \frac{\sum \theta_{i,j} / \boldsymbol{Y}_{i,j}}{N_i}$$

$\theta_{i,j}$: standard error of adjustment
$\boldsymbol{\Upsilon}_{i,j}$: data vector of mesured values for gene $i$ and brain $j$
$\boldsymbol{Y}_{i,j}$ : data vector of measured values for gene $i$ and brain $j$
$N_i$ : number of observations for gene $i$

The different $R^2$, PCV, and error values allow an evaluation of the model fit and the adjustment quality. $R^2$ coefficients could be regarded as a measure of variance explained by different aspects of the model, with values closer to one meaning better explanatory power. $R_i^2$ is closest to the *coefficient of determination* from standard linear regression, but should, according to [58], be supplemented by so-called *marginal (marg)* and *conditional (cond)* $R^2$ values, if a mixed effects model is evaluated. Since we are interested in the influence of fixed effects, $R^2_{\text{marg},i}$ is of special importance. The conditional coefficient $R^2_{\text{cond},i}$ additionally accounts for the influence of random effects. The difference between $R^2_{\text{cond},i}$ and $R^2_{\text{marg},i}$ gives insight to which extent inter-individual differences that are not explained by fixed effects are captured by the model through random effects. High PCV values express how well certain fixed effects are able to reduce the contribution of random effects to the explanatory power of the model. The relative adjustment error $\varepsilon_i$ gives the mean of the summed standard errors from adjustment in relation to the expression value for each gene $i$. Small values indicate low uncertainties by the adjustment procedure.

## 4 Notes

1. Ribonuclease contamination is a major concern for successful cDNA synthesis of single-laser microdissected cells or small cell pools. The ubiquitous RNase A is a highly stable and active ribonuclease, which is present on human skin as well as in the specimens, and can easily contaminate any lab environment. Thus, creating and maintaining an RNase-free work environment and RNase-free solutions is essential for performing successful reverse transcriptase reactions. Therefore, we strongly recommend: Always wear gloves when handling chemicals and sections/samples containing RNA. Change gloves frequently especially after touching potential sources of RNase contamination such as doorknobs, pens, pencils, and human skin. Always use certified RNase-free tubes, pipette tips and chemicals *for all steps* involved in the experiments (e.g., ethanol/staining solutions and jars for the preparation of tissue sections for UV-LMD). Keep chemicals tightly sealed. Keep all the tubes containing RNA tightly sealed during the incubation steps. Treat UV-LMD (membrane-) slides for 20 min with UVC-light (e.g., in a sterile hood). Heat sterilize all metal (forceps, spatulas, LMD cap holder, LMD slide holder), glassware and any other equipment that gets in contact with slides or reaction tubes during UV-LMD experiments at 220 °C overnight. Clean pipettes, benches, and all other equipment that cannot be heat sterilized with RNase decontamination solutions, e.g., RNase-ExitusPlus (AppliChem) and/or RNaseZapWipes (Ambion). Clean the cryostat additionally with isopropanol (Isopropanol, Sigma-Aldrich) to wipe off RNaseZap.
2. Low retention filter tips should be used for all pipetting steps.
3. We strongly recommend using chemicals from the same stocks and lots for all experiments of a study.
4. To avoid any RNase or DNA contamination, we recommend preparing the *Cap-Mix* under a sterile fume hood.
5. As RNA in human midbrain tissue is likely already partially degraded, we recommend using qPCR amplicon sizes below 80 bp when working with human tissue.
6. To reuse the specimen for several experiments, brains are fixed on cork discs with tissue freezing medium. These cork discs can be frozen quickly with a drop of water on the specimen holder of the cryostat and easily be removed after the experiment and stored again at −80 °C.
7. Tissue chippings of the cryosectioning procedure are used to assess overall RNA quality and tissue pH of each specimen.

Transfer chippings into a liquid nitrogen precooled Falcon tube with a cold forceps and store at −80 °C until further usage (e.g., pH-determination, or RNA extraction and small RNA, miRNA and RNA integrity number evaluation).

8. PEN-membrane slides with tissue sections can be stored in 50 ml Falcon tubes at −80 °C and reused for later experiments. To ensure that the slides stay dry, silica gel is added to the Falcon tube (Fig. 1). A small sieve is used to separate the silica gel from the slide. For reuse, the slides are removed from −80 °C and allowed to equilibrate at −20 °C (20 min), +4 °C (20 min), and finally at room temperature (20 min) before usage.
9. Our mild lysis protocols are optimized for single UV-laser microdissected cells or small pools of individual cells from ethanol-fixed tissue sections. Please note that they are neither suited for lysis of larger microdissected tissue samples, nor for lysis of single cells from PFA-fixed tissue sections.
10. Assay ID numbers for TaqMan assays (Life Technologies) are: SNCA: Hs00240906_m1, TH: Hs00165941_m1, DAT: Hs00997374_m1, VMAT2: Hs00996839_m1, NURR1: Hs00428691_m1, LDH-2: Mm00493146_m1, PITX3: custom assay, forward primer: GCACGGCTGCAAGGG, reverse primer: GGCTTCAGGTTCGTAGTCTTGAT; probe: FAM-ACCCTTCCTTGCCCAACTG-NFQ. Assay ID number for miR-133b SYBRGreen assay (Qiagen) is: MS00007385.

## Acknowledgments

We are particularly grateful to the brain donors, and the support by the German BrainNet (GA28, GA76 and GA82). We thank Falk Schlaudraff for providing most of the data shown here, Leica Microsystems for providing a UV-LMD6000 and Microdissect for providing PEN-membrane slides. This work was supported by the BMBF (NGFN 01GS08134), by the DFG (SFB497 and LI1745-1), the Austrian Science Fund (FWF SFB F4412), the Hertie Foundation, and the Alfried Krupp prize (all to BL). JD was supported by the PhD program for Molecular Medicine and the Research Training Group CEMMA (DFG) of Ulm University. JG is supported by an EMBO and Marie Curie Actions Fellowship as well as an SNF Ambizione Fellowship.

## References


1. Stahlberg A, Kubista M (2014) The workflow of single-cell expression profiling using quantitative real-time PCR. Expert Rev Mol Diagn 14:323–331
2. Bustin SA, Benes V, Garson JA et al (2009) The MIQE guidelines: minimum information for publication of quantitative real-time PCR experiments. Clin Chem 55:611–622
3. Saraiva LR, Ibarra-Soria X, Khan M et al (2015) Hierarchical deconstruction of mouse olfactory sensory neurons: from whole mucosa to single-cell RNA-seq. Sci Rep 5:18178
4. Chen J, Suo S, Tam PP et al (2017) Spatial transcriptomic analysis of cryosectioned tissue samples with Geo-seq. Nat Protoc 12:566–580
5. Ziegenhain C, Vieth B, Parekh S et al (2017) Comparative analysis of single-cell RNA sequencing methods. Mol Cell 65:631–643.e4
6. Gierahn TM, Wadsworth MH, Hughes TK et al (2017) Seq-Well: portable, low-cost RNA sequencing of single cells at high throughput. Nat Methods 14:395
7. AR W, Neff NF, Kalisky T et al (2014) Quantitative assessment of single-cell RNA-sequencing methods. Nat Methods 11:41–46
8. Saliba AE, Aj W, Gorski SA et al (2014) Single-cell RNA-seq: advances and future challenges. Nucleic Acids Res 42:8845–8860
9. Elowitz MB, Levine AJ, Siggia ED et al (2002) Stochastic gene expression in a single cell. Science 297:1183–1186
10. Dickson DW (2012) Parkinson's disease and parkinsonism: neuropathology. Cold Spring Harb Perspect Med 2:a009258
11. Lopez-Valdes HE, Martinez-Coria H (2016) The role of neuroinflammation in age-related dementias. Rev Invest Clin 68:40–48
12. Goedert M, Spillantini MG, Del Tredici K et al (2013) 100 years of Lewy pathology. Nat Rev Neurol 9:13–24
13. Braak H, Ghebremedhin E, Rüb U et al (2004) Stages in the development of Parkinson's disease-related pathology. Cell Tissue Res 318:121–134
14. Hindle JV (2010) Ageing, neurodegeneration and Parkinson's disease. Age Ageing 39:156–161
15. Surmeier DJ, Obeso JA, Halliday GM (2017) Selective neuronal vulnerability in Parkinson disease. Nat Rev Neurosci 18:101–113
16. Duda J, Potschke C, Liss B (2016) Converging roles of ion channels, calcium, metabolic stress, and activity pattern of Substantia nigra dopaminergic neurons in health and Parkinson's disease. J Neurochem 139 Suppl 1:156–178
17. Damier P et al (1999) The substantia nigra of the human brain. II. Patterns of loss of dopamine-containing neurons in Parkinson's disease. Brain 122:1437–1448
18. Damier P, Ec H, Agid Y et al (1999) The substantia nigra of the human brain. I. Nigrosomes and the nigral matrix, a compartmental organization based on calbindin D(28K) immunohistochemistry. Brain 122:1421–1436
19. Hirsch EC, Hunot S (2009) Neuroinflammation in Parkinson's disease: a target for neuroprotection? Lancet Neurol 8:382–397
20. Kalia LV, Lang AE (2015) Parkinson's disease. Lancet 386:896–912
21. Dachsel JC, Sj L, Gonzalez J et al (2007) The ups and downs of alpha-synuclein mRNA expression. Mov Disord 22:293–295
22. Cookson MR (2009) alpha-Synuclein and neuronal cell death. Mol Neurodegener 4:9
23. Anderegg A, Poulin JF, Awatramani R (2015) Molecular heterogeneity of midbrain dopaminergic neurons--moving toward single cell resolution. FEBS Lett 589(Pt A):3714–3726
24. Mariani E, Frabetti F, Tarozzi A et al (2016) Meta-analysis of Parkinson's disease transcriptome data using TRAM software: whole substantia nigra tissue and single dopamine neuron differential gene expression. PLoS One 11: e0161567
25. Markopoulou K, Biernacka JM, Armasu SM et al (2014) Does alpha-synuclein have a dual and opposing effect in preclinical vs. clinical Parkinson's disease? Parkinsonism Relat Disord 20:584–589
26. Hodne K, Weltzien FA (2015) Single-cell isolation and gene analysis: pitfalls and possibilities. Int J Mol Sci 16:26832–26849
27. Poulin JF, Zou J, DFrouin-Ouellet J et al (2014) Defining midbrain dopaminergic neuron diversity by single-cell gene expression profiling. Cell Rep 9:930–943
28. Baslan T, Hicks J (2014) Single cell sequencing approaches for complex biological systems. Curr Opin Genet Dev 26:59–65
29. La Manno G, Gyllborg D, Codeluppi S et al (2016) Molecular diversity of midbrain development in mouse, human, and stem cells. Cell 167:566–580.e19
30. Erickson HS, Albert PS, Gillespie JW et al (2009) Quantitative RT-PCR gene expression analysis of laser microdissected tissue samples. Nat Protoc 4:902–922
31. Murray GI (2007) An overview of laser microdissection technologies. Acta Histochem 109:171–176

32. Liss B, Roeper J (2004) Correlating function and gene expression of individual basal ganglia neurons. Trends Neurosci 27:475–481
33. Poetschke C, Dragicevic E, Duda J et al (2015) Compensatory T-type Ca2+ channel activity alters D2-autoreceptor responses of Substantia nigra dopamine neurons from Cav1.3 L-type Ca2+ channel KO mice. Sci Rep 5:13688
34. Dragicevic E, Poetschke C, Duda J et al (2014) Cav1.3 channels control D2-autoreceptor responses via NCS-1 in substantia nigra dopamine neurons. Brain 137:2287–2302
35. Krabbe S, Duda J, Schiemann J et al (2015) Increased dopamine D2 receptor activity in the striatum alters the firing pattern of dopamine neurons in the ventral tegmental area. Proc Natl Acad Sci U S A 112:E1498–E1506
36. Muhling T, Duda J, Weishaupt JH et al (2014) Elevated mRNA-levels of distinct mitochondrial and plasma membrane Ca(2+) transporters in individual hypoglossal motor neurons of endstage SOD1 transgenic mice. Front Cell Neurosci 8:353
37. Grundemann J, Schlaudraff F, Liss B (2011) UV-laser microdissection and mRNA expression analysis of individual neurons from postmortem Parkinson's disease brains. Methods Mol Biol 755:363–374
38. Schroeder A, Mueller O, Stocker S et al (2006) The RIN: an RNA integrity number for assigning integrity values to RNA measurements. BMC Mol Biol 7:3
39. Stan AD, Ghose S, Gao XM et al (2006) Human postmortem tissue: what quality markers matter? Brain Res 1123:1–11
40. Weis S, Llenos IC, Dulay JR et al (2007) Quality control for microarray analysis of human brain samples: the impact of postmortem factors, RNA characteristics, and histopathology. J Neurosci Methods 165:198–209
41. Lipska BK, Deep-Soboslay A, Weickert CS et al (2006) Critical factors in gene expression in postmortem human brain: focus on studies in schizophrenia. Biol Psychiatry 60:650–658
42. Tagliafierro L, Bonawitz K, Glenn OC et al (2016) Gene expression analysis of neurons and astrocytes isolated by laser capture microdissection from frozen human brain tissues. Front Mol Neurosci 9:72
43. Meyronet D, Dorey A, Massoma P et al (2015) The workflow from post-mortem human brain sampling to cell microdissection: a Brain Net Europe study. J Neural Transm (Vienna) 122:975–991
44. Trabzuni D, Ryten M, Walker R et al (2011) Quality control parameters on a large dataset of regionally dissected human control brains for whole genome expression studies. J Neurochem 119:275–282
45. Koppelkamm A, Vennemann B, Lutz-Bonengel S et al (2011) RNA integrity in post-mortem samples: influencing parameters and implications on RT-qPCR assays. Int J Leg Med 125:573–580
46. Schlaudraff F, Grundemann J, Fauler M et al (2014) Orchestrated increase of dopamine and PARK mRNAs but not miR-133b in dopamine neurons in Parkinson's disease. Neurobiol Aging 35:2302–2315
47. Eschbach J, von Einem B, Muller K et al (2017) Mutual exacerbation of PGC-1α deregulation and α-synuclein oligomerization. Ann Neurol 77:15–32
48. Grundemann J, Schlaudraff F, Haeckel O et al (2008) Elevated alpha-synuclein mRNA levels in individual UV-laser-microdissected dopaminergic substantia nigra neurons in idiopathic Parkinson's disease. Nucleic Acids Res 36:e38
49. Kurz A, Double KL, Lastres-Becker I et al (2010) A53T-alpha-synuclein overexpression impairs dopamine signaling and striatal synaptic plasticity in old mice. PLoS One 5:e11464
50. Ramirez A, Heimbach A, Grundemann J et al (2006) Hereditary parkinsonism with dementia is caused by mutations in ATP13A2, encoding a lysosomal type 5 P-type ATPase. Nat Genet 38:1184–1191
51. Schiemann J, Schlaudraff F, Klose V et al (2012) K-ATP channels in dopamine substantia nigra neurons control bursting and novelty-induced exploration. Nat Neurosci 15:1272–1280
52. Kim J, Inoue K, Ishii J et al (2007) A MicroRNA feedback circuit in midbrain dopamine neurons. Science 317:1220–1224
53. Matsuda-Matsumoto H, Iwazaki T, Kashern MA et al (2007) Differential protein expression profiles in the hippocampus of human alcoholics. Neurochem Int 51:370–376
54. McCullumsmith RE, Meador-Woodruff JH (2011) Novel approaches to the study of postmortem brain in psychiatric illness: old limitations and new challenges. Biol Psychiatry 69:127–133
55. Preece P, Cairns NJ (2003) Quantifying mRNA in postmortem human brain: influence of gender, age at death, postmortem interval, brain pH, agonal state and inter-lobe mRNA variance. Brain Res Mol Brain Res 118:60–71
56. Harrington CA, Winther M, Garred MM (2009) Use of bioanalyzer electropherograms for quality control and target evaluation in

microarray expression profiling studies of ocular tissues. J Ocul Biol Dis Inform 2:243–249

57. Consonni D, Bertazzi PA, Zocchetti C (1997) Why and how to control for age in occupational epidemiology. Occup Environ Med 54:772–776
58. Snijders TAB, Bosker RJ (2011) Multilevel analysis: an introduction to basic and advanced multilevel modeling, 2nd edn. Sage, London
59. Eschbach J, von Einem B, Muller K et al (2015) Mutual exacerbation of peroxisome proliferator-activated receptor gamma coactivator 1alpha deregulation and alpha-synuclein oligomerization. Ann Neurol 77:15–32
60. Liss B (2002) Improved quantitative real-time RT-PCR for expression profiling of individual cells. Nucleic Acids Res 30:e89
61. Ortner NJ et al (2017) Lower affinity of isradipine for L-type $Ca^{2+}$ channels during Substantia nigra dopamine neuron-like activity: implications for neuroprotection in Parkinson's disease. J Neurosci 37:6761
62. Liss B, Franz O, Sewing S et al (2001) Tuning pacemaker frequency of individual dopaminergic neurons by Kv4.3L and KChip3.1 transcription. EMBO J 20:5715–5724
63. Caguci DG (2003) Sensitivity and uncertainty analysis, Volume1: Theory. Chapman & Hall/CRC Press, New York, NY
64. Nakagawa S, Schielzeth H (2013) A general and simple method for obtaining R2 from generalized linear mixed-effects models. Methods Ecol Evol 4:133